

Network-aided Efficient LLM Services With Denoising-inspired Prompt Compression

Feiran You, Hongyang Du, Kaibin Huang, *Fellow, IEEE*, and Abbas Jamalipour, *Fellow, IEEE*

Abstract—Large Language Models (LLMs) have demonstrated remarkable capabilities in various tasks, leading to their increasing adoption in diverse services delivered through wireless networks. There is a growing trend toward longer prompts to better leverage LLMs' capabilities and address difficult tasks. However, longer prompts not only increase data transmission costs but also require more computing resources and processing time, which impacts overall system efficiency and user experience. To address this challenge, we propose Joint Power and Prompt Optimization (JPPO), a framework that combines Small Language Model (SLM)-based prompt compression with wireless power allocation optimization. By deploying SLM at edge devices for prompt compression and employing Deep Reinforcement Learning (DRL) for joint optimization of compression ratio and transmission power, JPPO effectively balances service quality with resource efficiency. Furthermore, inspired by denoising diffusion models, we design a denoising-inspired prompt compression approach that iteratively compresses prompts by gradually removing non-critical information, further enhancing the framework's performance. Experimental results with long prompt tokens demonstrate that our framework achieves high service fidelity while optimizing power usage in wireless LLM services, significantly reducing the total service response time. With our DRL-based JPPO, the framework maintains fidelity comparable to the no-compression baseline while still achieving a 17% service time reduction through adaptive compression. When prioritizing compression, our framework achieves a compression ratio of up to 16x while maintaining acceptable fidelity (within a 30% reduction). Compared to no compression, baseline single-round compression with a 16x compression ratio reduces the system total response time by approximately 42.3%, while the denoising-inspired method achieves a 46.5% service time saving.

Index Terms—Large language models, prompt engineering, power allocation, joint optimization

1 INTRODUCTION

Artificial intelligence (AI)'s rapid advancement has become a promising tool for enhancing 6G communication systems [1], [2], providing users with more diverse services. Large language models (LLMs) can offer capabilities to handle various tasks for the mobile users in the network and provide significant advantages in context-aware data processing, real-time inference, and efficient spectrum utilization, making them well-suited for next-generation networks like 6G [3]. Their ability to compress, interpret, and

F. You, H. Du, and K. Huang are with the Department of Electrical and Electronic Engineering, University of Hong Kong, Pok Fu Lam, Hong Kong SAR, China (email: fryou@eee.hku.hk, duhy@eee.hku.hk, huangkb@hku.hk). A. Jamalipour is with the School of Electrical and Computer Engineering, University of Sydney, Sydney, Australia (email: a.jamalipour@ieee.org). The conference version of this work has been accepted by the IEEE International Conference on Communications (ICC) 2025 [1].

generate relevant information with minimal latency significantly improves the performance of wireless communication systems, especially in resource-constrained environments. Additionally, LLMs have revolutionized natural language processing, demonstrating unprecedented capabilities across various tasks [4]. As these models increasingly drive intelligent IoT devices and edge computing applications, their deployment over wireless networks to provide services to end-users has become a critical scenario [5]. For instance, users can interact with LLM cloud assistants through their mobile devices, sending text queries over wireless networks to remote servers that host the models, which then process and return appropriate responses. However, this integration faces significant challenges from the computational demands of LLMs and the inherent constraints of wireless communication systems [6].

In LLM models, prompts act as input queries that direct the model's response generation, while tokens are the subword units the model processes to generate text [7]. These tokens are processed through a transformer architecture that consists of multiple layers of self-attention and feed-forward networks [8]. The model first tokenizes the input prompt into a sequence of tokens, which are then embedded and processed through the transformer layers to understand the context and generate appropriate responses. In wireless communication, efficient prompt compression can minimize bandwidth usage while preserving response fidelity. A key issue is the growing length of prompts used to elicit advanced reasoning from LLMs [9], particularly with the advent of techniques like In-Context Learning (ICL) [10] and Chain-of-Thought (CoT) prompting [11]. For example, users may need to upload lengthy documents along with their queries to enable LLMs to provide accurate answers, such as when asking the model to analyze a research paper or respond to a legal document containing thousands of words. While these methods substantially enhance LLM performance, they often necessitate prompts that can extend to tens of thousands of tokens [12]. This trend creates a fundamental trade-off: On the one hand, longer, more sophisticated prompts unlock the full potential of LLMs; on the other, they impose severe burdens on communication bandwidth and computing resources in wireless settings. Moreover, the inference latency significantly increases as longer prompts require more computational resources in the transformer architecture, where each token must attend to all previous tokens, resulting in quadratic complexity growth. This extended processing time delays the generation of the first output token, directly impacting the Quality of Service (QoS) by increasing the initial response time [13]. Consequently, the efficient deployment of LLMs in wireless networks demands innovative solutions that can balance

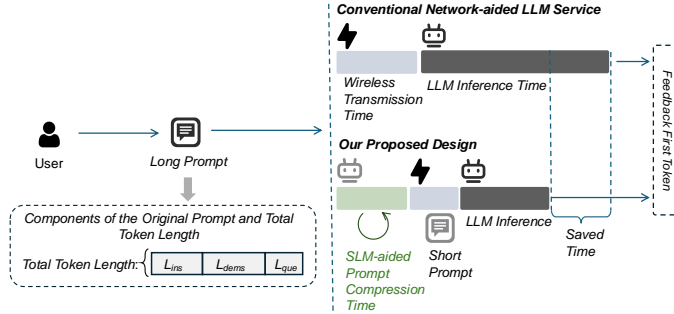


Fig. 1: Time consumption comparison of first token generation between conventional network-aided LLM inference service architecture and our design under long user prompts.

prompt inputs and resource efficiency requirements [14].

Prior research has tried to address these challenges from different angles. The authors in [15] introduced LLMLingua, a coarse-to-fine prompt compression method that demonstrates significant potential for compressing LLM prompts while preserving their semantic integrity. LLMLingua utilizes a small language model for compression, which can be aligned with the target LLM through instruction tuning. While this approach shows promise for reducing communication overhead, it does not fully account for the challenges posed by wireless transmission. The work in [16] proposes LLM-Slice, a system that creates dedicated network slices for LLM services to improve wireless resource management and reduce response delays. Although LLM-Slice advances wireless network architecture for LLM services, it focuses solely on communication resource allocation without considering prompt optimization for individual user requirements. Addressing these issues requires solving two key questions:

- **Q1**) How to achieve adjustable prompt compression without significantly degrading LLM inference performance and service quality?
- **Q2**) How to jointly design wireless resource allocation, particularly transmission power, to meet the latency and power consumption constraints of network-aided LLM services while maintaining high service quality?

For **Q1**, natural language processing methods offer potential solutions for prompt compression. However, traditional NLP compression techniques, such as text summarization or keyword extraction, often fail to capture the complex reasoning patterns and task-specific requirements embedded in LLM prompts, leading to degraded inference performance. Alternative AI-based approaches, such as large autoencoder models or specialized compression networks, require substantial computational resources and introduce additional inference latency at user terminals, making them impractical for resource-constrained wireless scenarios. Small Language Models (SLMs), which can be easily deployed at user terminals, offer a promising solution through their semantic understanding capability to compress LLM prompts while preserving task-critical information. SLM has been adapted as an effective way to employ transformers for edge applications in [17].

Furthermore, inspired by diffusion denoising models [18], we propose an iterative prompt compression algorithm as a complement to direct SLM-based compression. This approach views the refined, compressed prompt as a “noise-free” state and the original lengthy text as a “noisy” state. Similar to how diffusion models

progressively denoise images [18], our algorithm iteratively refines the text through multiple compression stages. This gradual approach addresses a key challenge: while directly compressing a long text might risk losing critical information, performing the compression in stages allows for more controlled information preservation. For instance, achieving a 16x compression through four iterations of 2x compression enables the model to process smaller, more manageable chunks of information at each step, reducing the risk of losing essential content. Despite the iterative nature, the computational overhead remains minimal due to SLM’s efficiency—our experiments show that each compression round only adds about 2% to the total LLM inference time.

Building upon this insight and addressing the **Q2**, we propose Joint Power and Prompt Optimization (JPPO), a framework that combines SLM-based prompt compression with wireless power allocation optimization, as illustrated in Fig. 1. JPPO captures the trade-off between compression ratio and wireless resource consumption, adapting to both channel conditions and prompt content. This integrated approach enables efficient wireless LLM services while maintaining response quality through intelligent prompt optimization. The contributions of this paper are summarized as

- We employ a small, aligned language model as a prompt compressor. This approach preserves useful information while significantly reducing the size of the prompt. The SLM efficiently captures essential meaning without requiring training at the transmitter. Additionally, we design a denoising-inspired prompt compression mechanism that performs compression through iterative refinement steps, further improving the system’s overall performance with marginal additional computational overhead.
- We formulate an optimization problem for our JPPO framework. This problem balances compression quality, wireless transmission performance, and LLM inference efficiency. The objective function is the QoS, considering energy limitation and end-to-end latency, with compression ratio and transmission power as key decision variables.
- To solve the complex JPPO optimization problem, we employ a Deep Reinforcement Learning (DRL) approach. The DRL agent learns to make optimal decisions on compression ratio and transmit power, effectively reducing communication overhead and accelerating LLM inference services in energy-constrained and variable wireless channel environments.

The remainder of this paper is organized as follows: Section 2 discusses related work in LLM deployment, prompt optimization, and wireless resource allocation. Section 3 presents our system model for wireless network-aided LLM services and introduces the novel denoising-inspired prompt compression method. Section 4 details the JPPO framework, including its mathematical foundations and implementation approach. Section 5 presents comprehensive numerical results and performance analysis. Finally, Section 6 concludes the paper with a summary of our key findings.

2 RELATED WORK

In this section, we discuss several related works, including LLMs, prompt compression, and wireless network management.

2.1 Large Language Models

The increasing adoption of wireless network-aided LLM-based services has enabled a range of applications, including real-time

decision-making and natural language processing services [19]. In [20], the authors proposed a comprehensive vision for designing universal foundation models tailored to the unique needs of next-generation wireless systems and promoted the design of Large Multi-modal Models (LMMs). Additionally, the growth of LLMs and their integration into wireless networks has significantly increased the demand for computational resources and communication bandwidth. Longer prompts exacerbate these challenges, especially in resource-constrained wireless environments, highlighting scalability issues. Efficient resource management is crucial for sustaining AI services in such limited network and computational conditions. In [21], the authors investigated an edge intelligence optimization problem tailored for LLM inference. They formulated an inference model for transformer decoder-based LLMs to maximize inference throughput through batch scheduling and joint allocation of communication and computation resources, while also considering edge resource constraints and varying user requirements for latency and accuracy. The authors in [22] introduced a novel LLM edge inference framework, incorporating batching and model quantization to ensure high-throughput inference on resource-limited edge devices. Then, they formulated an edge inference optimization problem based on the architecture of transformer decoder-based LLMs and solved the problem using the OT-GAH (Optimal Tree-search with Generalized Assignment Heuristics) algorithm. However, existing research on LLM overlooks the high latency caused by the increasing length of prompts in communication systems.

2.2 Prompt Compression

Prompt compression is a critical technique to mitigate the computational and communication overhead caused by the growing length of input prompts in LLM-based services. Current prompt compression methods face significant challenges due to the limitations of fine-tuning and inefficient compression processes [23]. These challenges include information loss, diminished model capability, and only marginal efficiency gains. In particular, conventional interference management strategies struggle when interference power approaches the level of signal power in wireless communication, leading to a degradation in overall system performance [24]. The authors of [25] proposed Variable Rate Cross-Modal Compression (VR-CMC) and introduced variable rate prompts to represent the data with different grains. In [26], the authors proposed a discrete prompt compression method using Prompt Compression with Reinforcement Learning (PCRL). And it used a computationally efficient policy network to edit prompts. The authors in [23] proposed an innovative framework that strategically tailors LLMs for streamlined context processing by harnessing the synergies among natural language summarization, soft prompt compression, and augmented utility preservation mechanisms. This framework reduces computational overhead and enhances the efficacy of LLMs across various benchmarks. However, prompt compression, combined with wireless power allocation optimization, has not been considered in prior studies. Prompt compression can reduce the data transmission load, while optimizing wireless power allocation ensures that the system operates within the power availability constraints. Jointly optimizing these two factors has the potential to significantly improve the performance and efficiency of wireless systems.

2.3 Wireless Network Management

Studies in wireless network management have made a significant impact, particularly in power allocation and joint optimization strategies. For power allocation, efficient solutions are crucial for maintaining network reliability under resource constraints. For instance, in [27], researchers developed an online Delayed-Interaction Collaborative-Learning Independent-Decision Multi-Agent DRL (DCLID-MADRL) algorithm that enables access points to independently optimize user selection and power configuration using only local information, thereby enhancing global energy efficiency. Recent studies have also demonstrated the effectiveness of joint optimization approaches in addressing complex wireless communication challenges. In [28], researchers simultaneously optimized multiple parameters, including receive beam-forming, power allocation, High-Altitude Platform Stations (HAPS) positioning, and computation resource distribution using block coordinate descent and successive convex approximation methods. Similarly, in [29], a Graph Neural Network (GNN)-based framework was proposed to jointly solve power control and spectrum allocation problems in a multi-interference environment with shared channels. However, despite these advancements in wireless network management and joint optimization techniques, a significant research gap remains in the context of network-aided LLM services.

In summary, despite the advancements in research discussed above, no existing studies have addressed power allocation strategies in scenarios involving LLM service delivery, particularly in terms of jointly optimizing prompt compression and transmission power for efficient network services. Compared to existing studies, we consider the novel JPPO framework, which combines SLM-based prompt compression with wireless power allocation optimization.

3 SYSTEM MODEL

In this section, we present the system model of wireless network-aided LLM inference services, the SLM-based prompt compression method, and the wireless transmission model with constraints on power consumption and delay.

3.1 Wireless Network-aided LLM Services

We consider a heterogeneous wireless network where a Data Center Operator (DCO) provides LLM inference services to N users with diverse task requirements, e.g., prompts. As illustrated in Fig. 2, our proposed framework consists of three key components: an SLM agent deployed at user devices or edge servers for prompt compression, a JPPO scheme for reliable wireless transmission, and a target LLM for inference service. On the user side, the SLM agent leverages its semantic understanding capability to compress prompts while preserving task-critical information. The compressed prompts are then transmitted through wireless channels with jointly optimized power allocation, and finally processed by the target LLM for inference. This framework adaptively adjusts both compression ratios and transmission power based on channel conditions and prompt characteristics to achieve high LLM service quality.

3.2 Prompt Compression

To efficiently reduce prompt sizes while preserving semantic integrity, we adopt a coarse-to-fine compression approach in SLMs.

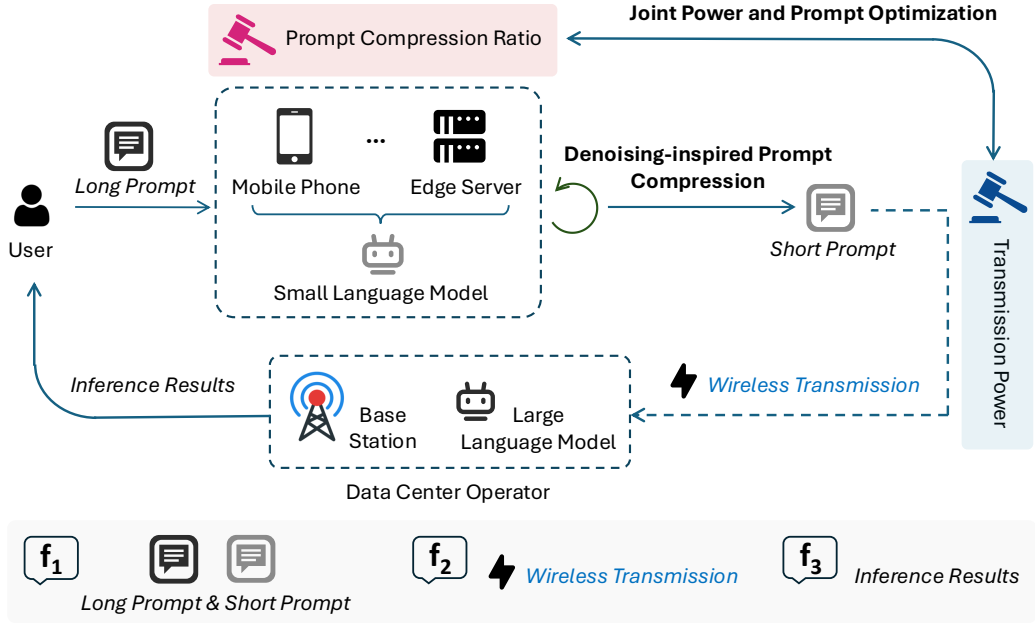


Fig. 2: System model of wireless network-aided LLM services and overview of our proposed JPPO, where user-generated long prompts are first compressed through SLM-based edge computing, then transmitted with optimized power allocation via wireless networks to the LLM server, and finally inference results are returned to users.

Our compression method is designed to achieve two primary objectives: preserving critical information in the prompt while ensuring the recoverability of the original semantic meaning, and enabling flexible compression ratios that can be dynamically adjusted together with communication resources.

Let us formally define the prompt structure and compression process. Consider an original prompt \mathbf{x} that consists of three components:

$$\mathbf{x} = (\mathbf{x}_{\text{ins}}, \mathbf{x}_{\text{dems}}, \mathbf{x}_{\text{que}}), \quad (1)$$

where \mathbf{x}_{ins} represents the instruction component, \mathbf{x}_{dems} denotes the demonstrations or examples, and \mathbf{x}_{que} contains the specific question or task. As depicted in Fig. 1, the token length of each component is denoted by \mathcal{L}_{ins} , $\mathcal{L}_{\text{dems}}$, and \mathcal{L}_{que} respectively. The total token length \mathcal{L}_x of the original prompt is given by:

$$\mathcal{L}_x = \mathcal{L}_{\text{ins}} + \mathcal{L}_{\text{dems}} + \mathcal{L}_{\text{que}}. \quad (2)$$

Our SLM-based compression mechanism generates a compressed prompt $\hat{\mathbf{x}}$ with length $\mathcal{L}_{\hat{x}}$. The compression ratio κ is defined as:

$$\kappa = \frac{\mathcal{L}_{\hat{x}}}{\mathcal{L}_x}, \quad \kappa \in [0, 1] \quad (3)$$

where $\kappa = 1$ indicates no compression and smaller κ represent higher compression rates.

We use a comprehensive fidelity metric \mathbf{f} capturing three essential aspects of semantic preservation during information transmission [30] to evaluate the quality of prompt compression. The fidelity metric is composed of three key components, as shown at the bottom of Fig. 2:

- *Representation accuracy* (\mathbf{f}_1), which measures how accurately the compressed prompt preserves the semantic meaning of the original prompt and maintains semantic integrity. \mathbf{f}_1 is measured by the overlap-based similarity metric based on the comparison between the representations of the original prompt and the compressed prompt. The computation of \mathbf{f}_1 is

to quantify the overlap between the tokens in the original and compressed prompts, calculate the number of overlapping tokens between the two prompts, and normalize it by dividing by the length of the original prompt.

- *Transmission completeness* (\mathbf{f}_2), which evaluates the integrity of information preservation during the compression process. \mathbf{f}_2 is calculated as the token retained in the compressed prompt compared to the original prompt, considering Bit Error Probability (BEP) in the wireless transmission of the user prompt. The computation \mathbf{f}_2 is obtained by multiplying the base fidelity by the channel effect. The base fidelity is calculated as the ratio of tokens retained in the compressed prompt to the number of tokens in the original prompt, adjusted by the compression ratio. Then, the channel effect is computed to reflect the impact of errors introduced by the channel.

- *Understanding accuracy* (\mathbf{f}_3), which quantifies how well the receiver (target LLM) can interpret the compressed prompt correctly. \mathbf{f}_3 is to evaluate the proximity of the response to the compressed prompt received and the predefined response to the original prompt, and is calculated as the number of overlapping tokens between the expected and original responses when prompt is not compressed, normalized by the length of the expected responses.

The overall fidelity metric \mathbf{f} can be defined as a weighted sum of these components:

$$\mathbf{f} = \alpha_1 \mathbf{f}_1 + \alpha_2 \mathbf{f}_2 + \alpha_3 \mathbf{f}_3, \quad (4)$$

where α_1 , α_2 , and α_3 are weight factors determining the relative importance of each fidelity component. These weights can be adjusted based on application requirements and QoS priorities.

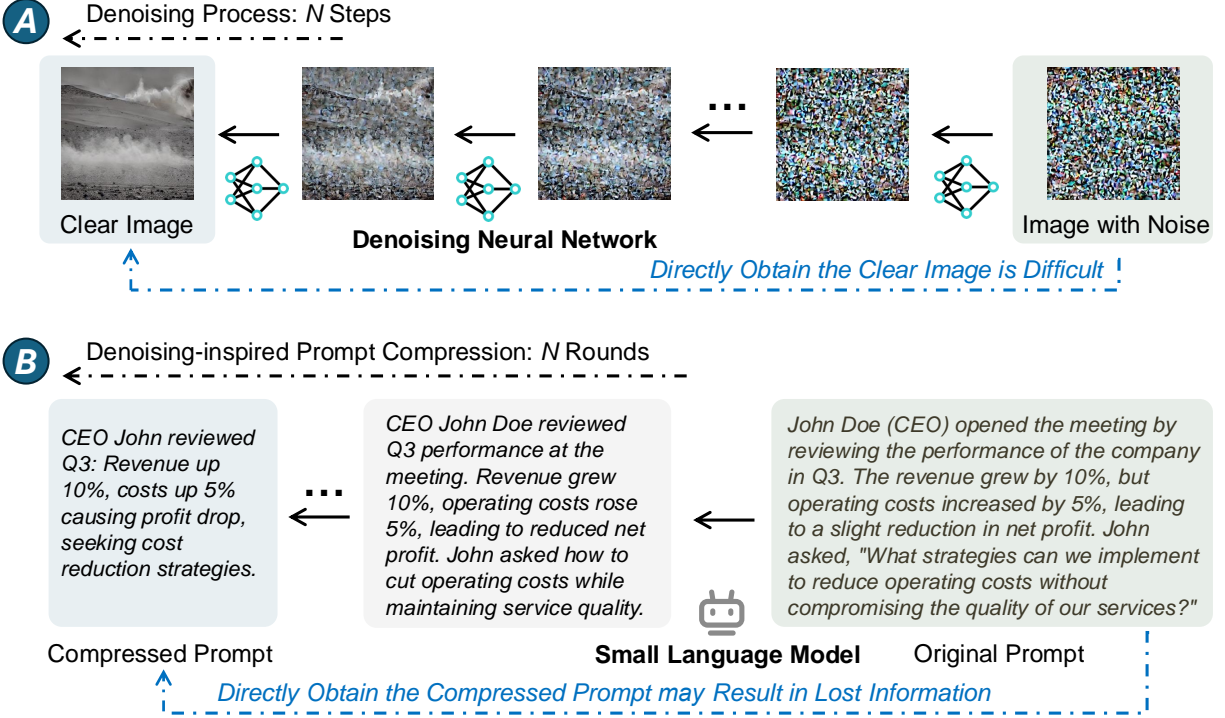


Fig. 3: The motivation of our proposed denoising-inspired prompt compression method. Part A demonstrates the process of DDPM-generating images through a denoising process. Rather than directly generating a clear image, the denoising neural network focuses on predicting noise one step at a time, using the image from the previous step to generate the current one. Part B illustrates the denoising-inspired prompt compression. Instead of directly obtaining a fully compressed prompt, SLM can also perform gradual prompt compression to reduce the degree of information that needs to be compressed in each round of processing, minimizing information loss.

3.3 Denoising-inspired Prompt Compression

We propose a framework for controlling the compression ratio across multiple steps, inspired by the denoising process in denoising diffusion models, e.g., Denoising Diffusion Probabilistic Models (DDPM) [18].

As shown in Part A of Fig. 3, in DDPM’s denoising process, the denoising network predicts the noise between the current state and the previous state, gradually removing noise through this process until a clean image is obtained. Compared to many AI algorithms that directly generate images, DDPM’s approach reduces training difficulty and improves image generation performance. Similarly, when we use SLM for text compression, the SLM continuously predicts the next token based on the input text to ultimately obtain the compressed prompt, as shown in Part B of Fig. 3. If we set a very high compression ratio all at once, the SLM might lose crucial information. However, if we consider denoising-inspired prompt compression, viewing the compressed prompt as a clean image and the original long prompt as a noisy state, we can enable the SLM to perform gradual prompt compression. During each compression step, we can select a relatively larger compression ratio, reducing the degree of compression, and achieve the same compression effect through multiple iterations. This way, during each compression step, the SLM needs to consider relatively less information to reduce, resulting in a lower probability of losing important information, as shown in Fig. 4 in Section 5. Although the iterative nature introduces additional SLM processing time, the system maintains its efficiency due to SLM’s swift operation—experiments in Section 5 show that each compression round only adds approximately 2% to the total

LLM inference time, while the optimized compression scheme can reduce subsequent LLM inference delay by around 40%.

Our method allows flexible scheduling of compression ratios while maintaining a deterministic path toward the target compression rate. Given the target compression ratio $T_\kappa = 1/\kappa$ (e.g., $T = 16$ for $16\times$ compression), we define a compression progress variable $t \in [0, 1]$, where $t = 0$ represents the original text and $t = 1$ represents the fully compressed text. The compression ratio at any time t is governed by:

$$\alpha(t) = T_\kappa^{-\sigma(t)} \quad (5)$$

where $\sigma(t)$ is a monotonically increasing scheduling function with $\sigma(0) = 0$ and $\sigma(1) = 1$. For a sequence of M compression steps, we discretize t into t_0, t_1, \dots, t_M , where $t_0 = 0$ and $t_M = 1$. The compression ratio between consecutive steps is given by:

$$\beta(i) = \frac{\alpha(t_i)}{\alpha(t_{i-1})} = T_\kappa^{-[\sigma(t_i) - \sigma(t_{i-1})]} \quad (6)$$

To enable flexible management of the compression process, We employ different scheduling methods tailored to various input prompt types, enabling flexible management of the compression process. The behavior of the compression process can be controlled through different choices of $\sigma(t)$:

- Linear schedule: The linear schedule is defined as

$$\sigma(t) = t. \quad (7)$$

This schedule applies a uniform compression rate throughout the entire process, ensuring consistent behavior across all steps, which is straightforward and computationally efficient.

- Cosine schedule: The cosine schedule is defined as

$$\sigma(t) = \frac{1 - \cos(\pi t)}{2}. \quad (8)$$

This schedule introduces smooth transitions at the beginning and end of the process. By tapering the compression rate during these stages, it minimizes abrupt changes, making it ideal for applications where gradual adjustments are critical to maintaining output quality.

- Quadratic schedule: The quadratic schedule is defined as

$$\sigma(t) = t^2. \quad (9)$$

This schedule concentrates the majority of compression in the later stages of the process, leaving earlier stages relatively unaffected, which would be effective for tasks requiring precise compression towards the final steps.

Note that different types of long prompts may require different optimal compression schedules. For a uniform N-step compression process with linear scheduling, the discrete time steps are given by $t_i = \frac{i}{M}$, where $i \in 0, 1, \dots, M$, with each step applying a constant compression ratio of $T_\kappa^{-1/M}$. The total compression at any time t satisfies $\alpha(t) \cdot \alpha(0) = T_\kappa^{-\sigma(t)}$. This formulation ensures that the initial state maintains the original length ($\alpha(0) = 1$), the final state achieves the target compression ($\alpha(1) = \frac{1}{T_\kappa}$), and the compression path remains continuously differentiable when using smooth scheduling functions. This framework provides a principled way to design multi-step compression strategies while maintaining precise control over the compression ratio at each step.

3.4 Energy Consumption

For one user, the total energy consumption E in the one-shot LLM service request process consists of two components: encoding energy E_e and transmission energy E_t . This can be expressed as:

$$E(\kappa, P_T) = E_e(\kappa) + E_t(\kappa, P_T), \quad (10)$$

where P_T is the transmit power. The encoding energy consumption E_e , which represents the energy used by the SLM encoder for prompt compression, is calculated as [31]

$$E_e = t_e^{\text{SLM}}(\kappa) n_{\text{gpu}}^{\text{SLM}} P_{\text{gpu}}^{\text{SLM}} + t_e^{\text{LLM}}(\kappa) n_{\text{gpu}}^{\text{LLM}} P_{\text{gpu}}^{\text{LLM}}, \quad (11)$$

where t_e^{SLM} represents the GPU execution time in SLM, n_{gpu} denotes the number of GPUs utilized, and P_{gpu} is the thermal design power per GPU, and superscript LLM denotes the corresponding parameters for the LLM.

The transmission energy consumption E_t is

$$E_t = t_t(\kappa) P_T = \frac{s(\kappa)}{R} P_T, \quad (12)$$

where s represents the bit length of the compressed prompt \hat{x} with compression ratio κ , and R is the transmission rate that can be expressed as

$$R = W \log_2 (1 + \gamma) = W \log_2 \left(1 + \frac{P_T g d^{-\alpha}}{\lambda^2} \right), \quad (13)$$

where W is the bandwidth of the offloading link between the user and DCO, γ is the Signal-to-Noise Ratio (SNR), g is the Rayleigh fading coefficient (exponentially distributed with unit mean), d represents the distance between user and DCO, α is the path-loss exponent, and λ^2 represents the Gaussian noise term in the Additive White Gaussian Noise (AWGN) channel.

3.5 Service Delay and Error

The total time consumption T comprises three components: encoding delay in SLM and LLM, and transmission delay, expressed as:

$$T(\kappa, P_T) = t_e^{\text{SLM}}(\kappa) + t_e^{\text{LLM}}(\kappa) + t_t(\kappa, P_T). \quad (14)$$

Beyond maintaining the delay within acceptable bounds, we must also consider potential service degradation caused by transmission errors in the wireless channel.

For wireless network-aided LLM services, user prompts must be uploaded to the LLM through a wireless environment. Due to potential bit errors during wireless transmission, these errors can directly affect the fidelity of the transmitted data. Therefore, it is crucial to consider the BEP to reflect the likelihood of the textural prompt being incorrectly received or decoded in the wireless system. For n_{th} user, the average BEP η can be given under various modulation formats by [32]

$$\text{BEP} = \int_0^\infty \frac{\zeta(\mu_2, \mu_1 \tau)}{2\zeta(\mu_2)} \varphi_{\tau_n}(\tau) d\tau, \quad (15)$$

where $\zeta(\cdot, \cdot)$ is the upper incomplete Gamma function [33, eq. (8.350.2)], φ represents the Probability Density Function (PDF) expression for wireless channel fading. $\zeta(\mu_2, \mu_1 \tau)/2\zeta(\mu_2)$ is the conditional bit-error probability, μ_1 and μ_2 are parameters specific to the modulation scheme, representing different combinations of modulation and detection techniques.

4 JOINT POWER AND PROMPT OPTIMIZATION

This section introduces the JPPO for wireless network-aided LLM services. After formulating the problem, we propose a Double Deep Q-Network (DQN) method [34] to address the joint optimization problem.

4.1 Problem Formulation

For our JPPO framework, we formulate an optimization problem that balances three key aspects: prompt compression quality, wireless transmission efficiency, and LLM service performance. The objective is to maximize the overall fidelity while satisfying power and latency constraints in the wireless network-aided LLM service system. Specifically, the joint optimization problem can be formulated as

$$\max_{\{\kappa, P_T\}} \mathbf{f}(\kappa, \eta(P_T)), \quad (16)$$

$$\text{s.t. } E(\kappa, P_T) \leq E_{\text{th}}, \quad (16a)$$

$$P_T \leq P_{\text{th}}, \quad (16b)$$

$$T \leq T_{\text{th}}, \quad (16c)$$

$$\mathbf{f} > \mathbf{f}_{\text{th}}, \quad (16d)$$

where P_{th} is the maximum allowable power consumption, T_{th} represents the maximum tolerable end-to-end latency, \mathbf{f}_{th} defines the minimum required fidelity. The constraints are designed to ensure practical system operation. Constraint (16a) is the energy constraint that represents the total energy budget limitation at the edge device side, introducing a critical trade-off: while higher transmission power P_T can lead to lower BEP η and thus improved wireless transmission fidelity \mathbf{f}_2 to enhance the overall fidelity \mathbf{f} , the energy constraint forces a higher compression ratio κ to reduce both the SLM/LLM inference energy cost and wireless transmission energy consumption; however, an excessively

high compression ratio can result in significant information loss from the original prompt, potentially degrading both the semantic preservation fidelity f_1 and LLM service quality fidelity f_3 . Constraint (16b) ensures the power consumption remains within the device's power budget, Constraint (16c) guarantees that the total service latency meets real-time requirements, Constraint (16d) maintains the quality of service by enforcing a minimum threshold on fidelity. This optimization framework allows us to find the optimal balance between compression ratio and transmission power while maintaining high-quality LLM service delivery.

4.2 Double DQN Solution

To solve the complex JPPPO optimization problem, we deploy a centralized Double DQN method to find optimal prompt compression and transmission strategies for N users, as shown in **Algorithm 1**. The centralized control of the DDQN agent ensures fairness by dynamically allocating bandwidth and power based on real-time user demands and varying channel conditions. The key elements of the proposed Double DQN design are

- **Environment:** The environment of the Double DQN algorithm in the proposed framework is the communication environment with N users.
- **State:** The state information includes the current fidelity of the transmitted message, SNR, and BEP. The state information of n_{th} user is captured in a 3-dimensional vector: $[\mathbf{f}_n(\eta_n), \gamma_n, \cdot]$.
- **Action:** The actions include selecting compression and power levels. The action space is denoted as $\mathcal{A} = \{\mathcal{A}_1, \dots, \mathcal{A}_N\}$, where \mathcal{A}_n is the action of n_{th} user and consists of a tuple with discrete values of compression ratio and transmission power level. The compression ratio level is discrete values range from 0 to 4. The transmission power level is discrete values ranging from 0 to 9, which affects BEP.
- **Reward:** The reward of the n_{th} user is \mathcal{R}_n , and in each episode, the agent accumulates rewards based on the actions. The reward function maximizes fidelity while minimizing penalties related to BEP and power usage.

The key design of the Double DQN is to decouple action selection from evaluation and address the over-estimation issue by using two separate networks: *Current Q-network*, which predicts Q-values based on the current state, and *Target Q-network*, which calculates target Q-values during updates and evaluates the Q-value of the best next action selected by the current Q-network, making the learning process of the Double DQN more stable.

The update steps of DQN are:

$$Q(s_t, a_t) \leftarrow Q(s_t, a_t) + \alpha r_{t+1} + \mu \max_a Q(s_{t+1}, a) - Q(s_t, a_t), \quad (17)$$

where $Q(s_t, a_t)$ is the estimated Q-value updated by the Bellman equation for taking action a_t in state s_t . α is the learning rate. r_{t+1} is the reward received after taking action a_t in state s_t and transitioning to state s_{t+1} . μ is the discount factor. $\max_a Q(s_{t+1}, a)$ is the maximum estimated Q-value for all possible actions in state s_{t+1} .

In DQN, the loss function is the Mean Squared Error (MSE) between the predicted Q-values and the target Q-values:

$$L_i(\theta_i) = \left[r_{t+1} + \mu \max_{a'} Q_{\text{target}}(s_{t+1}, a'; \theta_i^*) - Q(s_t, a_t; \theta_i) \right]^2, \quad (18)$$

Algorithm 1 Double DQN Algorithm

Input: Initialize the action space $\mathcal{A} = \{\mathcal{A}_1, \dots, \mathcal{A}_N\}$ and target privacy (ϵ, δ) .

Output: Reward.

- 1: *Initialization:* s_0 .
- 2: **for** each episode $k \in \{1, \dots, K\}$ **do**
- 3: Explore actions and obtain initial states.
- 4: **for** each step in the episode **do**
- 5: Take action a_t according to current policy.
- 6: Receive reward r_t and observe the next state s_{t+1} .
- 7: **if** s' is the final state **then**
- 8: $y = \mathcal{R}'$.
- 9: **else**
- 10: $y = \mathcal{R}' + [\alpha r_{t+1} + \gamma \max_a Q(s_{t+1}, a) - Q(s_t, a_t)]$.
- 11: **end if**
- 12: Sample a mini-batch of experiences from memory
- 13: **for** each experience (s, a, r, s') in the batch: **do**
- 14: Calculate target Q-values according to (13)
- 15: Compute the loss according to (12)
- 16: Perform gradient descent to minimize loss:
- 17: Update ϵ : $\epsilon = \max(\epsilon * \epsilon_{\text{decay}}, \epsilon_{\text{min}})$
- 18: Update the target Q-network every few episodes.
- 19: Accumulate total reward and update state:
- 20: Total reward $+ = r$, $s = s'$
- 21: **end for**
- 22: **end for**
- 23: **end for**
- 24: Update the policy parameter.
- 25: Terminate the training when the policy converges or after a predefined number of iterations.

where $L_i(\theta_i)$ is the loss for the i -th iteration with parameter θ_i . r_{t+1} and s_{t+1} are the reward and next state observed after taking action a_t in state s_t . $Q_{\text{target}}(s_{t+1}, a'; \theta_i^*)$ is the target Q-value estimated by the target network with parameters θ_i^* . $Q(s_t, a_t; \theta_i)$ is the predicted Q-value by the current Q-network with parameters θ_i .

The update steps of the Double DQN can be expressed as

$$y = r + \mu Q_{\text{target}} \left(s', \arg \max_{a'} Q(s', a'; \theta); \theta^- \right), \quad (19)$$

where $Q(s, a; \theta)$ is the estimated Q-value from the current Q-network with parameter θ and $Q_{\text{target}}(s', a'; \theta^-)$ is the Q-value from the target network with parameter θ^- .

5 NUMERICAL RESULTS

We design a customized environment with variable fidelity, SNR, and BEP to simulate the wireless network-aided LLM service framework. The centralized DQN agent manages the environment, which involves selecting compression and power levels. Its goal is to balance fidelity, minimize errors, and optimize power usage. The trained DRL model is designed with a modular architecture, making it adaptable to other types of networks and tasks. Its state representation, action selection, and reward mechanisms can be independently modified to accommodate communication networks. While the current implementation assumes a centralized optimization strategy, future work could explore decentralized and hybrid architectures to improve scalability and robustness. For instance, a distributed learning-based approach could allow multiple edge

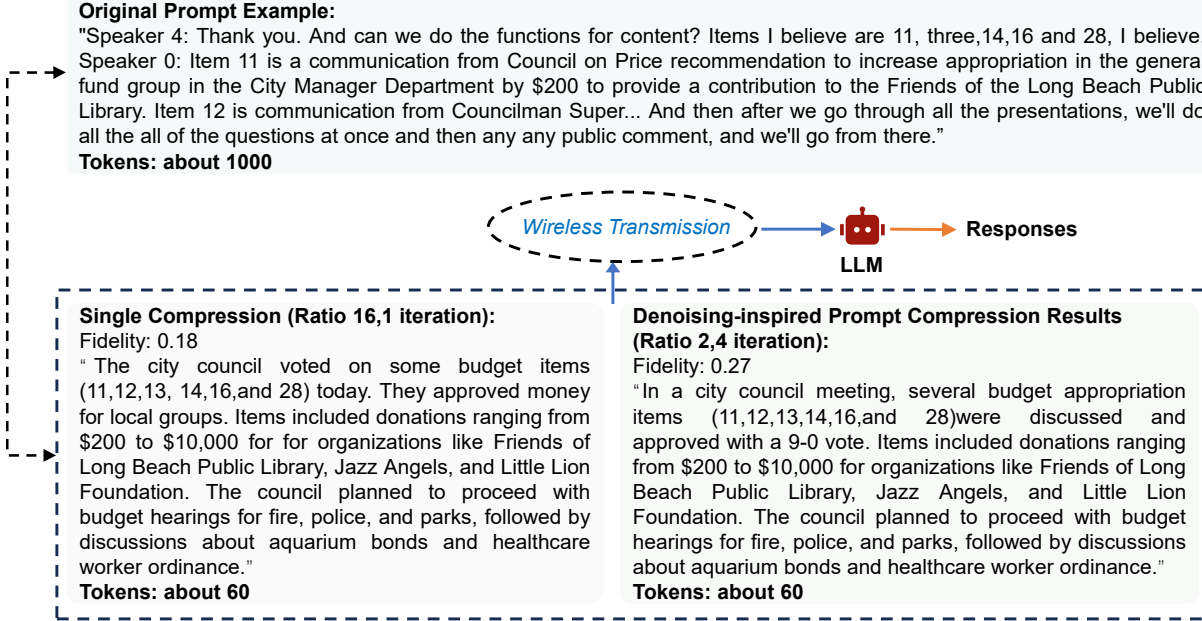


Fig. 4: The example illustrates wireless network-aided LLM services with SLM-based prompt compression, with a compression example of a single 16x compression ratio and an iterative 4 times 2x compression ratio.

TABLE 1: Simulation parameter configuration

Parameter	Value
Learning rate	10^{-3}
α_1 , α_2 , and α_3	0.4, 0.3 and 0.3
Total test runs range	[1, 10]
Episodes per test run	10,000

nodes to collaboratively optimize prompt compression and power allocation, thereby reducing the reliance on a single control unit. Moreover, integrating user-specific demands and heterogeneous network conditions into the optimization problem would allow for more adaptive and personalized service provisioning.

We use the LLMLingua platform, employing the SLM model with GPT-Neo 125M for prompt compression and GPT-J 6B to generate the response [35]. The simulations are carried out based on the MeetingBank-transcript dataset [36], where we select the long prompt data whose length exceeds 500 tokens from the dataset to apply in our system simulations. Other parameter settings are listed in Table 1.

The details of the datasets and experimental conditions are given as follows:

- **Network Conditions:** Our simulated MEC environment includes a total bandwidth of 20 MHz, a maximum transmission power of 10 dBm per user. Channel quality varies dynamically in the range of 0.1 to 1.
- **User Demand:** User task demands are randomly initialized, simulating heterogeneous data processing requirements.
- **Step Limit:** Each episode is capped at 100 steps to simulate practical usage constraints.
- **Random Seed:** To ensure reproducibility, we have initialized random seeds for both NumPy and PyTorch, ensuring consistency in experimental results.

Fig. 4 demonstrates prompt compression with a 16x com-

pression ratio. The iterative 4x2x compression ratio demonstrates superior efficiency compared to the single 16x compression ratio. It achieves a total power consumption of 8.18, with a reward score of 26.40. The compression process takes 2.92 seconds, followed by a response generation time of 2.48 seconds and a transmission time of 0.50 seconds, resulting in a total processing time of 5.90 seconds. In contrast, the single 16x compression ratio consumes significantly less total power at 2.90. However, it achieves a lower reward score of 17.74 and requires 6.59 seconds for compression, 4.12 seconds for response generation, and 0.55 seconds for transmission. This leads to a total processing time of 11.25 seconds, which is nearly twice as long as the iterative method. It shows that the iterative 4x2x compression ratio significantly reduces the total processing time while achieving a higher reward score, making it a more efficient compression strategy. The SLM significantly reduces the original prompt length while maintaining the accuracy of LLM responses, validating our SLM-based approach. Notably, our denoising-inspired prompt compression with linear scheduling preserves more key information and achieves higher fidelity metrics compared to single-step compression. Furthermore, our experimental results demonstrate the effectiveness of our wireless network-aided LLM services framework, using the selected MeetingBank-transcript dataset [36] (prompts > 500 tokens). First, when prioritizing maximum compression while maintaining acceptable fidelity, e.g., allowing up to 30% fidelity reduction, our framework achieved a compression ratio of up to 16x. At this compression level, compared to the no-compression baseline, we observed significant improvements in LLM service time. Specifically, the single-round baseline compression reduced service time by 42.3%, while our denoising-inspired prompt compression achieved an even better 46.5% reduction. Second, we evaluated our DRL-based JPPO approach, which optimizes the trade-off between compression and fidelity. The trained DRL model typically selected more conservative compression ratios

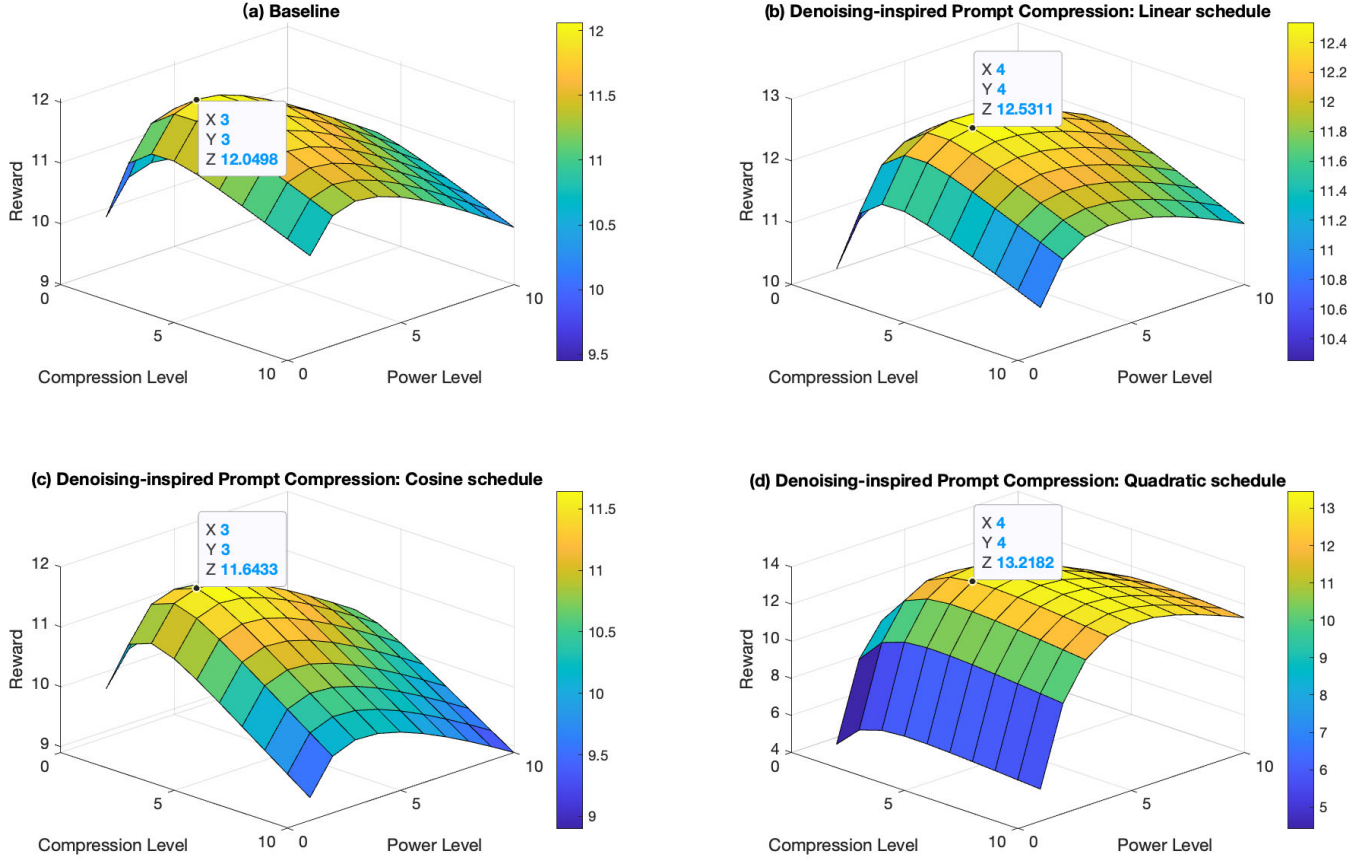


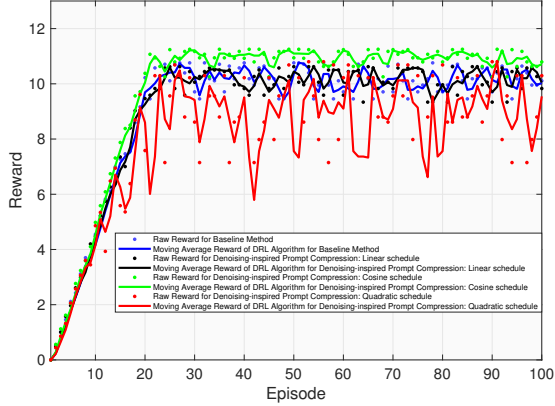
Fig. 5: One-shot reward values across different compression methods with respect to compression and power levels, tested using a single long prompt. Figs. 5 (a), (b), (c), and (d) show the reward performance of the baseline single-round compression method, the denoising-inspired prompt compression method with linear schedule, cosine schedule, and quadratic schedule, respectively.

(2–5x) to maximize fidelity. Even with these lower compression ratios, our framework maintained nearly identical fidelity while still achieving notable performance improvements. For example, for long prompts (approximately 600 tokens), the response time decreased from 85 to 71 seconds, representing a 17% speed improvement over the no-compression baseline. These results demonstrate that our framework can achieve aggressive compression with acceptable fidelity loss or maintain high fidelity while still delivering significant performance benefits.

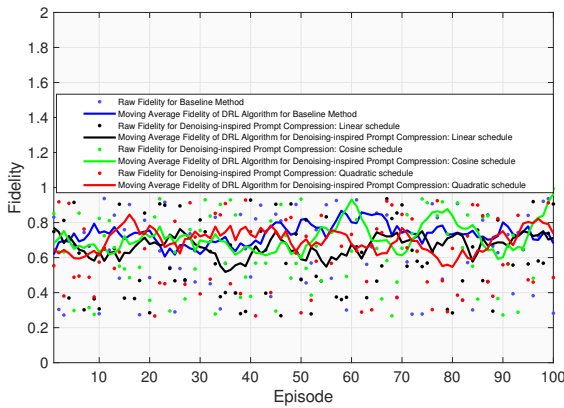
In Fig. 5, we present the end-to-end performance of LLM inference in wireless network-aided LLM services after SLM compression and wireless transmission for a specific long prompt. Specifically, Fig. 5 (a) shows the results of single-step 16x compression, while Fig. 5 (b), Fig. 5 (c), and Fig. 5 (d) demonstrate the effects of different denoising-inspired prompt compression schedules (linear, cosine, and quadratic, respectively) under the same compression requirements. For each approach, the reward grid plot illustrates the relationship between compression levels (1–10) and power levels (1–10). We observe that the optimal rewards of the baseline compression method are achieved at moderate compression levels (2–5) to achieve high fidelity scores and moderate power levels (2–5) because of the energy constraint. Key insights from our analysis reveal an important trade-off between prompt compression ratio and transmit power. While higher compression ratios can reduce textural prompt volume and subsequent LLM inference time, allowing for relatively higher transmit power under

energy constraints to reduce BEP, there is a risk of compromising performance due to loss of critical information affecting fidelity. Conversely, lower compression ratios maintain longer textural prompts but restrict transmit power settings, potentially increasing BEP and resulting in higher delays for LLM processing of longer prompts, leading to less noticeable performance gains. Another crucial insight is the variation in maximum achievable rewards across different denoising-inspired prompt compression schedules. For our test prompt, the optimal schedule demonstrates over 10% improvement in reward value compared to single-step compression, which can translate to noticeably better inference results and reduced delay from the user's perspective. This suggests that selecting an appropriate compression scheme based on the prompt's context type after establishing a compression ratio requirement can be highly effective.

Fig. 6 demonstrates the training effects on long prompts exceeding 500 tokens from the MeetingBank-transcript dataset [36]. Specifically, Fig. 6 (a) illustrates the reward convergence patterns across different compression methods, showing how the Double DQN method effectively learns optimal policies for compression and power allocation. The cosine schedule demonstrates superior performance for meeting transcripts, as its smooth transitions (defined by $\sigma(t) = \frac{1-\cos(\pi t)}{2}$) are particularly well-suited for maintaining the coherence and context of conversational data. This effectiveness is especially notable for meeting transcripts, where the cosine schedule's moderate compression steps at the



(a) The convergence performance of reward over 100 iterations for the DRL algorithm.



(b) The performance of fidelity over 100 iterations for the DRL algorithm.

Fig. 6: Performance metrics (i.e., reward and fidelity) of the DRL algorithm.

beginning and end, with more aggressive compression in the middle stages, helps preserve both the meeting’s contextual flow and key discussion points. Fig. 6 (b) tracks the average fidelity across episodes, comparing different compression schedules and showing stabilization around 0.7, which indicates robust information preservation even with significant compression. This high fidelity, combined with improved rewards, suggests our method successfully balances prompt compression levels and transmission power allocation, achieving efficient wireless network-aided LLM services while maintaining an acceptable average BEP.

Fig. 7 plots the performance when running with the LongBench dataset and compares the scores gained by no compression method, a single compression method with a single 16x compression ratio, and an iterative compression method with an iterative 4 times 2x compression ratio. The comparison is conducted from the perspective of both the average QA F1 score [37] and the Rouge-L score [38] using the Multi-news and Govreport data types. The F1 score evaluates question-answering systems, with higher values indicating better performance. A score of 1 indicates perfect classification, while a score of 0 means complete misclassification. It balances precision and recall. ROUGE-L assesses text generation quality by comparing outputs to reference texts. The ‘L’ stands for Longest Common Subsequence (LCS), which captures matching

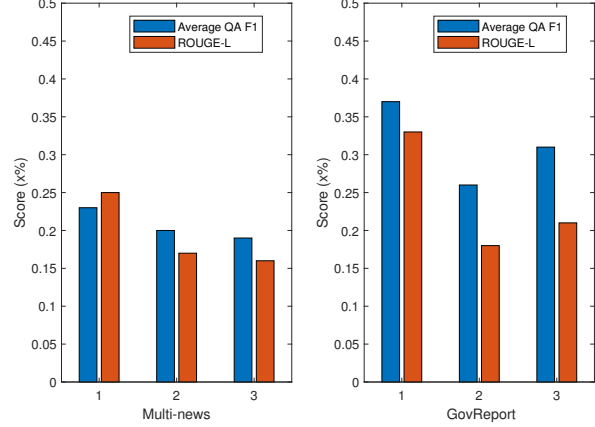


Fig. 7: The score performance when running with the LongBench dataset.

sequences in order, though not necessarily consecutively. It is observed from the figure that for the multi-news category, the no compression, single compression, and iterative compression methods achieve similar scores. In the govreport category, the iterative compression method achieves higher scores in both the F1 score and ROUGE-L score.

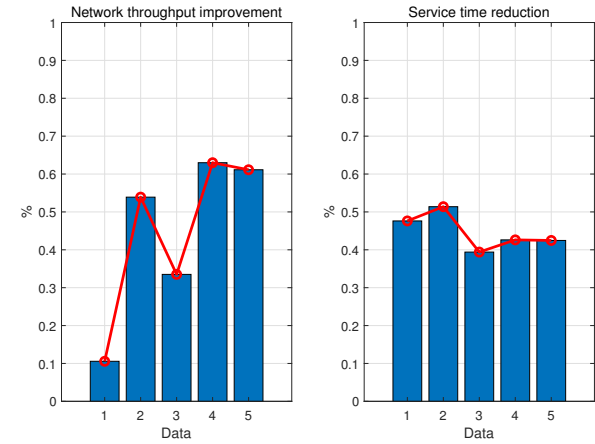


Fig. 8: The illustration of network throughput improvement and service time reduction. Network throughput improvement corresponds to the reduction in transmission time, and service time includes the compression time, transmission time, and inference time as shown in Fig. 1.

Fig. 8 plots the network throughput improvement and service time reduction with 5 data examples randomly sampled from the MeetingBank-transcript dataset. The network throughput improvement is the reduction in transmission time of the compressed prompt, showing the decrease in transmission time using the proposed denoising-inspired prompt compression method compared to the single compression method. The service time is the sum of the compression time, transmission time and inference time as shown in Fig. 1. The ratio in the figure shows the reduction of service time using the proposed denoising-inspired prompt compression method compared with the single compression method. It shows that the proposed denoising-inspired prompt compres-

sion method can consistently enhance network throughput while simultaneously reducing service time. The results indicate that this approach effectively optimizes data transmission efficiency, ensuring faster response times without compromising performance. This consistent improvement highlights the method's robustness in handling different data types and network scenarios, making it a reliable solution for efficient network communication.

6 CONCLUSION AND FUTURE DIRECTION

We proposed a novel joint power and prompt optimization framework for wireless network-aided accelerated LLM services. Additionally, inspired by denoising diffusion models, we designed a denoising-inspired prompt compression scheme to further enhance system performance. The proposed approach delivers high service quality with a relatively low BEP while keeping power consumption within limits. Numerical results show that the proposed algorithm demonstrates stable convergence, highlighting its suitability for practical deployment in LLM service systems.

Several promising directions for future research emerge from this work. While our current implementation treats the denoising-inspired prompt compression scheduling type and the iteration count as fixed parameters to demonstrate performance improvements, these could be incorporated as optimization variables in future studies. Different text types may benefit from different compression schedules, and the number of iterations, being directly linked to computing resources and system performance, could be integrated into the optimization problem. The ability to optimize both power and prompt compression makes this approach well-suited for resource-constrained environments, such as autonomous systems, industrial IoT, and smart home networks. These domains require efficient data transmission and minimal latency, aligning well with our proposed method. Additionally, integrating adaptive prompt compression with real-time processing in edge computing can enhance system performance while maintaining power efficiency. Furthermore, the deployment of SLMs at edge devices, facilitated by their small parameter count, opens up new research opportunities regarding their role in communication networks and their interaction with LLMs.

REFERENCES

- [1] F. You, H. Du, K. Huang, and A. Jamalipour, "JPPO: Joint power and prompt optimization for accelerated large language model services," *arXiv preprint arXiv:2411.18010*, 2024.
- [2] W. Xu, Y. Huang, W. Wang, F. Zhu, and X. Ji, "Toward ubiquitous and intelligent 6g networks: From architecture to technology," *Science China Information Sciences*, vol. 66, no. 3, p. 130300, 2023.
- [3] G. Zhu, Z. Lyu, X. Jiao, P. Liu, M. Chen, X. U. Jie, S. Cui, and P. Zhang, "Pushing AI to wireless network edge: an overview on integrated sensing, communication, and computation towards 6G," *SCIENCE CHINA Information Sciences*, vol. 66, no. 3, p. 130301, 2023.
- [4] B. Min, H. Ross, E. Sulem, A. P. B. Veyseh, T. H. Nguyen, O. Sainz, E. Agirre, I. Heintz, and D. Roth, "Recent advances in natural language processing via large pre-trained language models: A survey," *ACM Computing Surveys*, vol. 56, no. 2, pp. 1–40, 2023.
- [5] O. Friha, M. Amine Ferrag, B. Kantarci, B. Cakmak, A. Ozgun, and N. Ghoualni-Zine, "LLM-based edge intelligence: A comprehensive survey on architectures, applications, security and trustworthiness," *IEEE Open Journal of the Communications Society*, vol. 5, pp. 5799–5856, 2024.
- [6] F. Jiang, Y. Peng, L. Dong, K. Wang, K. Yang, C. Pan, D. Niyato, and O. A. Dobre, "Large language model enhanced multi-agent systems for 6G communications," *IEEE Wireless Communications*, 2024.
- [7] R. Patil and V. Gudivada, "A review of current trends, techniques, and challenges in large language models (llms)," *Applied Sciences*, vol. 14, no. 5, p. 2074, 2024.
- [8] S. Qian, Y. Zhu, W. Li, M. Li, and J. Jia, "What makes for good tokenizers in vision transformer?" *IEEE Transactions on Pattern Analysis and Machine Intelligence*, vol. 45, no. 11, pp. 13 011–13 023, 2023.
- [9] B. Xiao, B. Kantarci, J. Kang, D. Niyato, and M. Guizani, "Efficient prompting for LLM-based generative internet of things," *IEEE Internet of Things Journal*, pp. 1–1, 2024.
- [10] T. Li, G. Zhang, Q. D. Do, X. Yue, and W. Chen, "Long-context LLMs struggle with long in-context learning," *arXiv preprint arXiv:2404.02060*, 2024.
- [11] J. Wei, X. Wang, D. Schuurmans, M. Bosma, F. Xia, E. Chi, Q. V. Le, D. Zhou *et al.*, "Chain-of-thought prompting elicits reasoning in large language models," *Adv. Neural Inf. Process. Syst.*, vol. 35, pp. 24 824–24 837, 2022.
- [12] F. Xue, Y. Fu, W. Zhou, Z. Zheng, and Y. You, "To repeat or not to repeat: Insights from scaling LLM under token-crisis," *Adv. Neural Inf. Process. Syst.*, vol. 36, 2024.
- [13] M. Xu, H. Du, D. Niyato, J. Kang, Z. Xiong, S. Mao, Z. Han, A. Jamalipour, D. I. Kim, X. Shen *et al.*, "Unleashing the power of edge-cloud generative ai in mobile networks: A survey of aigc services," *IEEE Communications Surveys & Tutorials*, 2024.
- [14] O. Friha, M. A. Ferrag, B. Kantarci, B. Cakmak, A. Ozgun, and N. Ghoualni-Zine, "LLM-based edge intelligence: A comprehensive survey on architectures, applications, security and trustworthiness," *IEEE Open Journal of the Communications Society*, 2024.
- [15] H. Jiang, Q. Wu, C.-Y. Lin, Y. Yang, and L. Qiu, "LLMLingua: Compressing prompts for accelerated inference of large language models," *arXiv preprint arXiv:2310.05736*, 2023.
- [16] B. Liu, J. Tong, and J. Zhang, "LLM-Slice: Dedicated wireless network slicing for large language models," in *Proc. ACM Conf. Embedded Netw. Sensor Syst.*, 2024, pp. 853–854.
- [17] M. Scherer, L. Macan, V. J. B. Jung, P. Wiese, L. Bompani, A. Burrello, F. Conti, and L. Benini, "DeepDeploy: Enabling energy-efficient deployment of small language models on heterogeneous microcontrollers," *IEEE Transactions on Computer-Aided Design of Integrated Circuits and Systems*, vol. 43, no. 11, pp. 4009–4020, 2024.
- [18] J. Ho, A. Jain, and P. Abbeel, "Denoising diffusion probabilistic models," *Advances in neural information processing systems*, vol. 33, pp. 6840–6851, 2020.
- [19] J. Shao, J. Tong, Q. Wu, W. Guo, Z. Li, Z. Lin, and J. Zhang, "Wireless-LLM: Empowering large language models towards wireless intelligence," *Journal of Communications and Information Networks*, vol. 9, no. 2, pp. 99–112, 2024.
- [20] S. Xu, C. Kurisummoottil Thomas, O. Hashash, N. Muralidhar, W. Saad, and N. Ramakrishnan, "Large multi-modal models (LMMs) as universal foundation models for AI-native wireless systems," *IEEE Network*, vol. 38, no. 5, pp. 10–20, 2024.
- [21] X. Zhang, J. Liu, Z. Xiong, Y. Huang, G. Xie, and R. Zhang, "Edge intelligence optimization for large language model inference with batching and quantization," in *2024 IEEE Wireless Communications and Networking Conference (WCNC)*, 2024, pp. 1–6.
- [22] X. Zhang, J. Nie, Y. Huang, G. Xie, Z. Xiong, J. Liu, D. Niyato, and X. S. Shen, "Beyond the cloud: Edge inference for generative large language models in wireless networks," *IEEE Transactions on Wireless Communications*, pp. 1–1, 2024.
- [23] C. Wang, Y. Yang, R. Li, D. Sun, R. Cai, Y. Zhang, and C. Fu, "Adapting LLMs for efficient context processing through soft prompt compression," in *Proceedings of the International Conference on Modeling, Natural Language Processing and Machine Learning*, 2024, pp. 91–97.
- [24] Z. Meng, Q. Li, A. Pandharipande, and X. Ge, "Prompt-assisted semantic interference cancellation on moderate interference channels," *IEEE Wireless Communications Letters*, vol. 13, no. 10, pp. 2847–2851, 2024.
- [25] J. Gao, J. Li, C. Jia, S. Wang, S. Ma, and W. Gao, "Cross modal compression with variable rate prompt," *IEEE Transactions on Multimedia*, vol. 26, pp. 3444–3456, 2024.
- [26] H. Jung and K.-J. Kim, "Discrete prompt compression with reinforcement learning," *IEEE Access*, vol. 12, pp. 72 578–72 587, 2024.
- [27] Z. Wang, L. Zhang, D. Feng, G. Wu, and L. Yang, "Intelligent cloud-edge collaborations for energy-efficient user association and power allocation in space-air-ground integrated networks," *IEEE Journal on Selected Areas in Communications*, vol. 42, no. 12, pp. 3659–3673, 2024.
- [28] X. Yu, X. Zhang, Y. Rui, K. Wang, X. Dang, and M. Guizani, "Joint resource allocations for energy consumption optimization in HAPS-aided MEC-NOMA systems," *IEEE Journal on Selected Areas in Communications*, vol. 42, no. 12, pp. 3632–3646, 2024.
- [29] M. Marwani and G. Kaddoum, "Graph neural networks approach for joint wireless power control and spectrum allocation," *IEEE Transactions on*

Machine Learning in Communications and Networking, vol. 2, pp. 717–732, 2024.

[30] P. A. Stavrou and M. Kountouris, “The role of fidelity in goal-oriented semantic communication: A rate distortion approach,” *IEEE Transactions on Communications*, vol. 71, no. 7, pp. 3918–3931, 2023.

[31] A. Faiz, S. Kaneda, R. Wang, R. Osi, P. Sharma, F. Chen, and L. Jiang, “LLMCarbon: Modeling the end-to-end carbon footprint of large language models,” in *prof. Int. Conf. Learn. Represent.* ICLR, 2024.

[32] D. Tse and P. Viswanath, *Fundamentals of wireless communication*. Cambridge university press, 2005.

[33] I. S. Gradshteyn and I. M. Ryzhik, *Table of Integrals, Series, and Products*, 7th ed. Academic Press, 2007.

[34] H. Van Hasselt, A. Guez, and D. Silver, “Deep reinforcement learning with double q-learning,” in *Proceedings of the AAAI conference on artificial intelligence*, vol. 30, no. 1, 2016.

[35] D. Rothman, *Transformers for Natural Language Processing: Build, train, and fine-tune deep neural network architectures for NLP with Python, Hugging Face, and OpenAI’s GPT-3, ChatGPT, and GPT-4*. Packt Publishing Ltd, 2022.

[36] Y. Hu, T. Ganter, H. Deilamsalehy, F. Dernoncourt, H. Foroosh, and F. Liu, “Meetingbank: A benchmark dataset for meeting summarization,” in *Proceedings of the 61st Annual Meeting of the Association for Computational Linguistics (ACL)*. Toronto, Canada: Association for Computational Linguistics, 2023.

[37] R. Fakoor, A. Kainth, S. Shakeri, C. Winestock, A.-r. Mohamed, and R. Sarikaya, “Direct optimization of f-measure for retrieval-based personal question answering,” in *2018 IEEE Spoken Language Technology Workshop (SLT)*. IEEE, 2018, pp. 815–822.

[38] C.-Y. Lin, “Rouge: A package for automatic evaluation of summaries,” in *Text summarization branches out*, 2004, pp. 74–81.